Checkerboard and stripe inhomogeneities in cuprates

G. Seibold,[1] J. Lorenzana,[2] and M. Grilli[3]

[1]*Institut für Physik, BTU Cottbus, PBox 101344, 03013 Cottbus, Germany*
[2]*SMC-INFM, ISC-CNR, Dipartimento di Fisica, Università di Roma "La Sapienza," P. Aldo Moro 2, 00185 Roma, Italy*
[3]*INFM-SMC Center and Dipartimento di Fisica, Università di Roma "La Sapienza," P. Aldo Moro 5, I-00185 Roma, Italy*
(Received 16 January 2007; published 29 March 2007)

We systematically investigate charge-ordering phases by means of a restricted and unrestricted Gutzwiller approximation to the single-band Hubbard model with nearest- (t) and next-nearest- (t') neighbor hopping. When $|t'/t|$ is small, as appropriate for La$_{2-x}$Sr$_x$CuO$_4$, stripes are found, whereas in compounds with larger $|t'/t|$ (such as Ca$_{2-x}$Na$_x$CuO$_2$Cl$_2$ and Bi$_2$Sr$_2$CaCu$_2$O$_{8+\delta}$) checkerboard structures are favored. In contrast to the linear doping dependence found for stripes the charge periodicity of checkerboard textures is locked to 4 unit cells over a wide doping range. In addition we find that checkerboard structures are favored at surfaces.

The presence of charge and related spin inhomogeneities in underdoped high-temperature superconducting cuprates has received substantial experimental support.[1–4] Less clear is the symmetry of the underlying textures, an issue which is strongly debated.[4–7]

Neutron scattering experiments on lanthanum cuprates (LCO) are usually interpreted in terms of one-dimensional modulations (stripes) where the two-dimensional symmetry of the scattering is explained with the presence of orthogonal stripe domains.[5] Indeed, a substantial anisotropy in the *dynamic* scattering between the two planar axis, as expected for fluctuating stripes, has been explicitly demonstrated in studies on untwinned samples of YBa$_2$Cu$_3$O$_y$ (YBCO).[4,6] On the other hand, scanning tunneling microscopy (STM) in other classes of cuprates—namely, the bilayer Bi$_2$Sr$_2$CaCu$_2$O$_{8+\delta}$ (Bi-2212) (Ref. [8–11]) and the single-layer Ca$_{2-x}$Na$_x$CuO$_2$Cl$_2$ (Na-CCOC) (Ref. [12])—has revealed two-dimensional modulations (checkerboards). The peculiar characteristics of the Fermi surface of Na-CCOC (Ref. [13]) is also in agreement with the expected features of a disordered checkerboard phase.[14]

Charge-ordering (CO) phenomena thus seem to be common (and possibly generically present) in cuprates but the different symmetries found are rather puzzling and make one wonder if one should not reinterpret the neutron scattering experiments in LCO and YBCO in terms of two-dimensional textures also.[7]

CO was predicted in cuprates before any experimental detection.[15] However, its cooperation or competition with superconductivity is still debated. In this regard a possible direct relation between T_c and the intensity of incommensurate low-energy scattering[16] demands a deeper understanding of the physical mechanisms inducing CO and of the symmetry of the textures.

In this work we address this issue on the basis of the one-band Hubbard Hamiltonian. It has been argued that within this model, the ratio between nearest- (t) and next-nearest- (t') neighbor hopping $t'/t < 0$ is the main electronic parameter characterizing the different cuprate families.[17,18] We find a transition from one-dimensional to two-dimensional textures as $|t'/t|$ is increased. In addition, we find that the tendency to form checkerboard structures is in-

creased at surfaces. Our results provide a clue to interpret the contrasting experimental results regarding the symmetry of CO structures in different cuprate compounds.

We solve the Hubbard model within an unrestricted Gutzwiller approximation (GA). The GA energy is minimized with respect to unconstrained charge, spin, and double-occupancy distributions (for details see Ref. [19]). Generally we restrict ourselves to solutions without spin canting but we have checked the results lifting this restriction in several cases. In the case of stripes, once the unrestricted solution has been found, the symmetry of the solution has been imposed on a supercell and the problem has been solved in momentum space, allowing one to obtain smooth curves of the energy as a function of doping. In the other cases, the curves are not smooth due to restricted sampling, but we estimate that the finite-size corrections to the energy of single points are negligible due to the large size of the cells (up to 16×16).

The use of the present mean-field-like scheme to address the phenomenon of CO in cuprates requires further justification: (i) Previous studies have shown that the GA applied to a three-band Hubbard model and in the present model captures the phenomenology of stripes in LCO cuprates.[20] In particular it accounts for the behavior of incommensurability and of the chemical potential as a function of doping. This requires an accurate evaluation of the small energy difference between different stripe solutions. (ii) Response functions, due to fluctuations on top of these mean-field states, are in good agreement with spectroscopies,[21,22] both in the charge[23] and in the spin sector.[24] (iii) The accuracy of the charge distributions can be directly tested comparing with exact methods. We have found that the charge profile in the GA is indistinguishable from density matrix renormalization group computations[25] revealing stripes on a 7×6 Hubbard cluster doped with four holes. (iv) Finally, the charge profile predicted within the GA in the three-band Hubbard model[20] has recently been found to be in excellent agreement with a charge-sensitive measurement.[3]

All this establishes the GA as a very reliable technique to determine charge inhomogeneities in a strongly correlated system. In our computations we assume long-range order whereas in experiments this is rarely the case and stripes are assumed to be dynamical. (Glassy stripes are also a likely
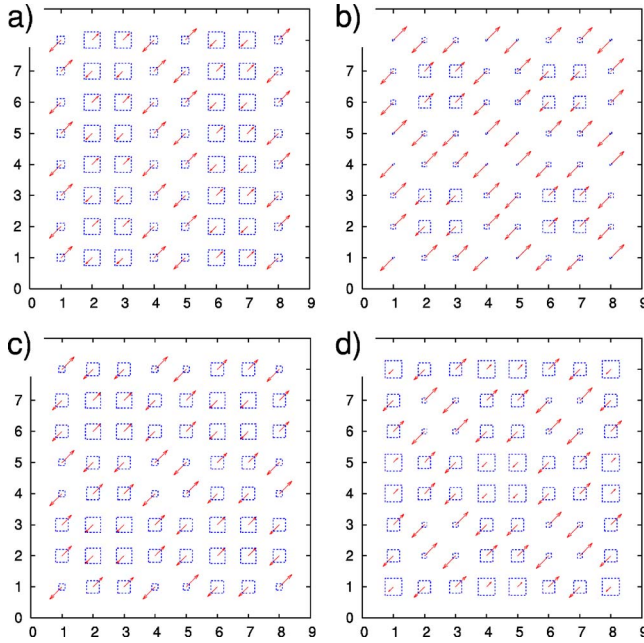
FIG. 1. (Color online) CO textures for $U/t=8$. The length of arrows is proportional to the spin density whereas the squares are proportional to the hole density minus the hole density in the insulator. (a) Bond-centered stripe texture with charge spacing $d=4$, doping $n_h=1/8$, and $t'/t=-0.2$; (b) SF checkerboard with $d=4$ at $x=0.06$ and $t'/t=-0.5$; (c) same as (b) with $n_h=1/8$; (d) LF checkerboard with $d=4$ and $t'/t=-0.5$ at $n_h=1/8$.

possibility that is usually neglected.) In any case the ground-state energy contains short-range correlations and is rather insensitive to the presence or absence of long-range order which justifies our approach.[20(a)]

For LCO we fix the Hubbard on-site repulsion $U/t=8$ and $t'/t=-0.2$. This parameter set and a very similar one reproduce the spectrum of magnetic excitations both in the undoped and doped phases.[24] The Hubbard interaction U and the nearest-neighbor hopping are not expected to depend significantly on the material given the similarity of superexchange interactions.[18] Instead t' has been found to be quite sensitive to the cuprate family.[17,18] Photoemission studies in the insulating parent compounds have shown that there is substantial splitting among states with momentum $(\pi/2, \pi/2)$ and $(\pi, 0)$ (we set the lattice constant $a \equiv 1$). Detailed studies of a single hole in one-band models suggest that this splitting roughly scales with t'.[18] Taking $t'/t=-0.2$ for LCO,[24] we estimate t' in Bi-2212 and CCOC by rescaling t' with the observed splitting.[18] In this way we obtain $t' \sim -0.4t$ for Bi-2212 and $t' \sim -0.5t$ for CCOC. The increase of $|t'/t|$ from LCO to Bi-2212 is in agreement with local density approximation (LDA) results[17] whereas for CCOC the present semiempirical estimate is significantly larger.

Figure 1 shows the most relevant textures found in this study: (a) is the bond-centered (BC) stripe solution already reported in previous studies[20] (b)–(d) are checkerboard textures. At low doping (n_h) and for large values of $|t'/t|$ we find the configuration (b) to be particularly stable. It can be seen as a lattice of ferromagnetic (FM) polarons or "ferrons" and is referred to as small ferron checkerboard (SFC). Each
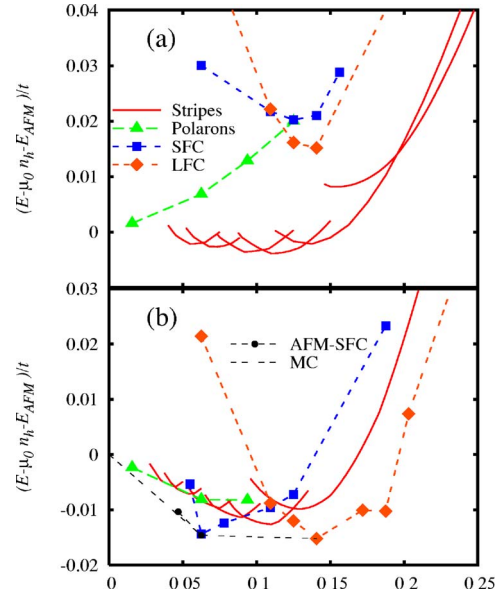

FIG. 2. (Color online) Energy per site as a function of doping for the different textures studied and for $t'/t=-0.2$ (a) and $t'/t=-0.5$ (b). For clarity we subtracted the energy of the AFM solution and the line $\mu_0 n_h$ with $\mu_0=-1.6t$. Different choices of μ_0 correspond to different choices of the origin of the energy of the single-particle states and do not change the physics. In each curve for the stripes the charge periodicity perpendicular to the stripe is fixed and takes the values (from left to right) $d=10,8,6,5,4,3$. In panel (b) we also show the energies allowing for spin canting and AFM-SFC mixing (solid circles) and Maxwell construction (MC) for AFM-SFC phase separation and for SFC and LFC phase separation.

ferron consists of a 2×2 plaquette with uniform magnetization and resides at the intersections of a crossed array of antiphase domain walls of the antiferromagnetic (AFM) order parameter. As doping increases the domain walls populate more uniformly and evolve into a configuration that resembles a crossed array of stripes (c). At higher doping the size of the ferromagnetic islands increases, producing a large ferron checkerboard (LFC) structure (d). In addition, we have considered arrays of spin polarons (not shown) consisting of single spin flips which locally bind the holes.

Fourier transforming the charge and spin distributions, we find that the most intense Bragg peaks for the $d=4$ checkerboards (SFC, LFC) are at $\mathbf{Q}_c=(\pm\pi/2,0), (0, \pm\pi/2)$ (charge) and at $\mathbf{Q}_s=(\pi\pm\pi/4, \pi\pm\pi/4)$ (spin). The rotation between $\mathbf{Q}_c$ and $\mathbf{Q}_s$ is in agreement with Ref. 5 and characterizes this kind of checkerboard. For stripes one finds no rotation [$\mathbf{Q}_c=(0\pm 2\pi/d,0)$ and $\mathbf{Q}_s=(\pi\pm\pi/d,0)$ for stripes along y]; however, also checkerboard patterns with no rotation are conceivable.

In Fig. 2 we report the values of the energy per site, E, for selected checkerboard (dashed lines) and stripe (solid lines) textures in the case of $t'/t=-0.2$ (a) and $t'/t=-0.5$ (b). The main general conclusion one can draw from Fig. 2 is that a sizable value of the next-nearest-neighbor hopping t' stabilizes checkerboard solutions with respect to stripes, which are more stable at small $|t'/t|$. This is the most generic and relevant finding of this work and provides a rationale as to
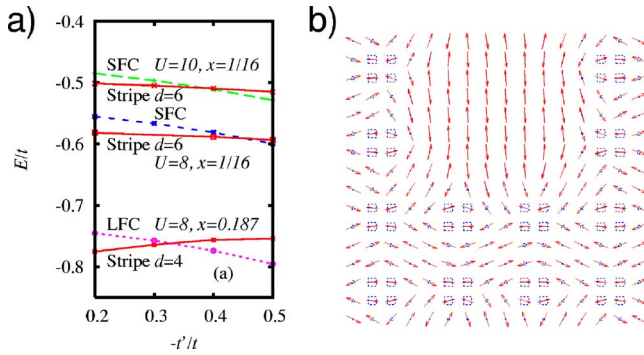
a)

b)

FIG. 3. (Color online) (a) Energy per site vs $-t'/t$ for $U/t = 8, 10$ for stripes and checkerboard at $n_h = 0.0625, 0.187$. (b) Mixed AFM-SFC solution at $n_h = 0.047$ and allowing for spin canting.

why stripes are observed in LCO materials (where $t'/t \approx -0.2$), while STM experiments detect checkerboard structures in Na-CCOC and Bi-2212, where t'/t is known to be substantially larger.[18]

Figure 3(a) gives details of this issue by comparing the energy of checkerboard with stripe solutions as a function of t'/t. Although most of the CO structures gain energy by increasing $|t'|$, it is clearly apparent that the checkerboard solutions take a much greater advantage from this increase and become more stable at $|t'/t| > 0.33-0.45$ depending on doping. Adding a third nearest-neighbor hopping (not shown) $t'' = -0.5t'$ (Ref. 17) does not change much this result. In this case the transitions occur in the range $0.36 < |t'/t| < 0.41$.

Bond-centered checkerboards take advantage from the "ferronic" nodes of the charge texture, while site-centered checkerboards (not shown) lack this important feature and have much higher energies. This is a major difference with respect to stripe structures, where bond-centered and site-centered textures are nearly degenerate. Another important difference lies in the doping dependence of the periodicity. The most stable stripe solution at low doping (cf. Fig. 2) has $d \sim 1/(2n_h)$ (with $d \approx 4-10$) providing an explanation[20] for the well-known linear behavior between doping and incommensurability.[2] In contrast, the bond-centered checkerboards lose (magnetic) energy in the domain walls and it is more convenient for them to adjust the charge in the FM plaquettes, keeping the domain walls as short as possible. Indeed the checkerboard structures with $d > 4$ (not shown) are at higher energy in the whole doping range. This provides an explanation for the fact that in Na-CCOC the charge periodicity is independent of doping and locked at $d = 4$.[12] For Bi-2212 $d \approx 4-4.7$ (Refs. 9–11) has been reported in STM experiments. However, here the interpretation is more difficult due to the presence of lattice modulations, mesoscopic inhomogeneities, and less pronounced CO peaks.

The SFC is particularly stable for large $|t'/t|$ at $n_h = 1/16 \sim 0.06$ [cf. Fig. 2(b)] when each ferron accommodates one added hole. This finding can be substantiated from an estimate of the electronic energy of an isolated 2×2 plaquette. One obtains the eigenvalue structure $-2t - t'; t'; t'; 2t - t'$ with the last level unoccupied due to the

presence of the hole. This yields the energy per site, $E - E_{AFM} = J\alpha - t(1 - t'/2t)/8$, where $-J\alpha$ is the energy per bond of the AFM phase. Additional carriers have to overcome a large gap $(2t - 2t')$, leading to a rapid rise of the energy (cf. Fig. 2). At $n_h = 1/16$ other configurations take a smaller advantage from $t'/t < 0$ while the magnetic energy cost is higher in the checkerboard. Therefore a substantial value of $|t'/t|$ is needed to stabilize checkerboards with respect to stripes and polarons.

At higher doping and for large $|t'|$ it pays to break more AFM bonds to have larger ferromagnetic islands to accommodate the holes. In this sense the SFC and LFC states locally reflect the tendency of the extended Hubbard model towards ferromagnetism for large $|t'|$ (Refs. 26 and 27) and can be seen as inhomogeneous precursors of the uniform ferromagnetic phase, although they do not have a net ferromagnetic moment. There is no evidence yet that checkerboard patterns have local ferromagnetic tendencies, so our results are predictive in this regard. Interestingly, after this work was posted an unpublished work appeared which on the basis of experimental evidence also suggests that ferromagnetism may play an increasingly important role as doping is increased.[28]

At intermediate dopings $n_h \sim 0.1$ and $t'/t = -0.5$ a phase-separated solution between the SFC and LFC has lower energy than $d = 4$ stripes. Ignoring the long-range Coulomb interaction the energy of this solution is given by the Maxwell construction [dashed line labeled MC in Fig. 2(b)]. This solution will be frustrated in the presence of the long-range Coulomb interaction, giving rise to a mesoscopic phase separation.[29] However, since the solutions are similar, they can be mixed at a quite small length scale which implies a low Coulomb cost.

At doping $n_h < 1/16$ the SFC is expected to phase separate with the AFM solution. MC for this case is also shown in Fig. 2(b) while the corresponding charge and spin distribution for $n_h = 0.047$ is shown in Fig. 3(b). In this case the two phases are quite different which can imply a high energy cost for mesoscopic phase separation[29] since a large surface energy may be expected at the interface. We have found, on the contrary, that allowing for spin canting one finds a solution with negligible surface energy cost as shown by the solid circle at $n_h = 0.047$ in Fig. 2(b). Indeed, although the solutions have a substantial amount of interface due to the finiteness of the cluster [Fig. 3(b)], the energy is very close to the MC line, for which the surface energy cost is assumed to be zero. This is because the surface energy is dominated by magnetic effects, but spin twisting allows for a smooth "flipping" of the magnetic order parameter from the SFC to the pure AFM in accord with standard arguments for an order parameter which breaks a continuous symmetry.[30] We also see from Fig. 2(b) that for the pure checkerboard solution at $n_h = 1/16$ the spin canting energy gain is negligible.

Mesoscopic textures like the one shown in Fig. 3(b) will also be influenced by disorder effects which will randomly pin clusters of one or the other phase according to their charge. It is clear from Fig. 3(b) that this will also induce substantial disorder on the spin degrees of freedom providing a natural mechanism for spin-glass effects often seen in underdoped cuprates.

As in previous studies we find that with a ratio of $|t'/t|$ appropriate for LCO the more stable inhomogeneities are stripes. As $|t'/t|$ is increased checkerboard structures are favored. Bi-2212 and Na-CCOC are estimated to lie close to the transition[31] providing an explanation for the puzzling difference in symmetry observed. The limited accuracy of specific parameter estimates and of the critical $|t'/t|$ for checkerboard structures does not allow one to exclude stripes in the bulk of these materials. Quantum fluctuations may also blur the difference among different configurations close to the transition.

So far checkerboard textures have only been detected by surface sensitive probes but are not yet established as a bulk phenomenon. Quite generally at the surface one may expect that screening of Coulomb interactions[32] is less effective, leading to an increase of U. Increasing the value to $U/t=10$ we find [cf. Fig. 3(a)] that checkerboard structures are more favored with respect to stripes and the critical value of $|t'/t|$ is decreased by about 15%. It is thus possible that checkerboard structures are an example of electronic surface reconstruction and occur only at surfaces.[33]

In conclusion, we have shown that the next-nearest-neighbor hopping plays a dominant role in determining the symmetry of CO textures in cuprates. Whereas for a ratio $t'/t=-0.2$ as appropriate for LCO we find stripes as the most stable inhomogeneities, a crossover to checkerboard solutions occurs for large but still realistic values of $|t'/t|$. Checkerboards behave quite differently as a function of doping with respect to stripes in that the periodicity of the modulation is locked as observed experimentally.[12] The competition between FM clusters and antiphase domains rules the relative stability of the various textures. Spin canting produces a negligible energy gain for ordered structures but it is fundamental for nanoscopically mixed phases.

A change of symmetry from stripes in the bulk of LCO and YBCO to checkerboards at the surface of Bi-2212 and Na-CCOC appears quite naturally, thereby explaining the puzzling lack of universality found for the symmetry of CO. On the other hand, CO itself appears to be quite ubiquitous in cuprates.

[1] J. M. Tranquada *et al.*, Nature (London) **375**, 561 (1995).

[2] K. Yamada *et al.*, Phys. Rev. B **57**, 6165 (1998).

[3] P. Abbamonte *et al.*, Nat. Phys. **1**, 155 (2005).

[4] H. A. Mook *et al.*, Nature (London) **404**, 729 (2000).

[5] J. M. Tranquada, Physica B **241**, 745 (1998).

[6] V. Hinkov *et al.*, Nature (London) **430**, 650 (2004).

[7] B. V. Fine, Phys. Rev. B **70**, 224508 (2004).

[8] J. E. Hoffman *et al.*, Science **295**, 466 (2002).

[9] C. Howald *et al.*, Phys. Rev. B **67**, 014533 (2003).

[10] M. Vershinin *et al.*, Science **303**, 1995 (2004).

[11] K. McElroy *et al.*, Phys. Rev. Lett. **94**, 197005 (2005).

[12] T. Hanaguri *et al.*, Nature (London) **430**, 1001 (2004).

[13] K. M. Shen *et al.*, Science **307**, 901 (2005).

[14] G. Seibold *et al.*, Eur. Phys. J. B **13**, 87 (2000).

[15] J. Zaanen and O. Gunnarsson, Phys. Rev. B **40**, 7391 (1989); K. Machida, Physica C **158**, 192 (1989); H. J. Schulz, Phys. Rev. Lett. **64**, 1445 (1990); D. Poilblanc and T. M. Rice, Phys. Rev. B **39**, 9749 (1989); U. Löw *et al.*, Phys. Rev. Lett. **72**, 1918 (1994); C. Castellani, C. Di Castro, and M. Grilli, *ibid.* **75**, 4650 (1995).

[16] S. Wakimoto *et al.*, Phys. Rev. Lett. **92**, 217004 (2004); Phys. Rev. B **60**, R769 (1999).

[17] E. Pavarini *et al.*, Phys. Rev. Lett. **87**, 047003 (2001).

[18] K. Tanaka *et al.*, Phys. Rev. B **70**, 092503 (2004).

[19] G. Seibold, Phys. Rev. B **58**, 15520 (1998).

[20] (a) J. Lorenzana and G. Seibold, Phys. Rev. Lett. **89**, 136401 (2002); (b) G. Seibold and J. Lorenzana, Phys. Rev. B **69**, 134513 (2004).

[21] J. M. Tranquada *et al.*, Nature (London) **429**, 534 (2004).

[22] S. Uchida *et al.*, Phys. Rev. B **43**, 7942 (1991).

[23] J. Lorenzana and G. Seibold, Phys. Rev. Lett. **90**, 066404 (2003).

[24] G. Seibold and J. Lorenzana, Phys. Rev. Lett. **94**, 107006 (2005); Phys. Rev. B **73**, 144515 (2006); J. Lorenzana, G. Seibold, and R. Coldea, *ibid.* **72**, 224511 (2005).

[25] S. R. White and D. J. Scalapino, Phys. Rev. Lett. **91**, 136403 (2003).

[26] T. Tohyama and S. Maekawa, Phys. Rev. B **49**, 3596 (1994).

[27] T. Hanisch, G. S. Uhrig, and E. Müller-Hartmann, Phys. Rev. B **56**, 13960 (1997).

[28] A. Kopp, A. Ghosal, and S. Chakravarty, cond-mat/0606431 (unpublished).

[29] J. Lorenzana, C. Castellani, and C. Di Castro, Phys. Rev. B **64**, 235127 (2001); Europhys. Lett. **57**, 704 (2002); C. Ortix, J. Lorenzana, and C. Di Castro, Phys. Rev. B **73**, 245117 (2006).

[30] Y. Imry and S. Keng Ma, Phys. Rev. Lett. **35**, 1399 (1975).

[31] The case of YBCO is more difficult because $|t'/t|$ is probably larger than in LCO, but orthorhombicity is more pronounced and requires a more specific calculation.

[32] J. van den Brink *et al.*, Phys. Rev. Lett. **75**, 4658 (1995); M. B. J. Meinders *et al.*, Phys. Rev. B **52**, 2484 (1995).

[33] S. Okamoto and A. J. Millis, Nature (London) **428**, 630 (2004).